Study on the mechanical capacity and structural relevance of a flying buttress through the analysis of a particular case

Albert Samper[a]* Rodrigo Martín-Sáiz [b] and David Moreno-García[b]

[a]*Institut de Recerca Històrica, Universitat de Girona, Girona, Spain;* [b]*Escola Tècnica Superior d'Arquitectura, Universitat Rovira i Virgili, Tarragona, Spain*

albert.samper@urv.cat* (corresponding author)

Albert Samper is an architect who obtained his Ph.D. in Architecture at the University of Rovira i Virgili in 2014. Presently, he is an assistant professor of architecture at the same university and his main fields of interest are: architectural heritage, architectural representation and the application of geometry to architecture. Presenly, he is doing a second doctoral thesis in the doctoral program entitled "Doctoral Program in Humanities, Heritage and Cultural Studies" at the University of Girona.

Rodrigo Martín-Sáiz is an architect who obtained his Ph.D. in Architecture at the Polytechnic University of Catalonia in 2015. Presently, he is an adjunct professor of architecture at the University of Rovira i Virgili and his main field of interest is the analysis of architectural structures.

David Moreno is an architect and Ph D student at the University of Rovira i Virgili in 2019. Presently, he is an Associate professor of architecture at the same university and his main fields of interest are architectural heritage and architectural representation. He has collaborated in the realization of the three-dimensional modelling, with point cloud techniques, of the Cathedral of Mallorca, the Cathedral of Girona and the Cathedral of Narbona.

Study on the mechanical capacity and structural relevance of a flying buttress through the analysis of a particular case

A flying buttress serves an aesthetic purpose and two technical purposes. In particular, it helps to drain rainwater from the roof and also plays a structural role. The aesthetic and drainage functions can be determined visually and with the help of several bibliographical references. On the contrary, in order to assess the structural function a rigorous mechanical study must be carried out. Starting from the mechanical capacity of a flying buttress, this paper presents a method to determine its relevance and influence on the structural behaviour of the cathedral.

Keywords: Flying buttress; Culée; Mechanical analysis; Gothic architecture; Girona Cathedral

Subject classification codes: include these here if the journal requires them

1. Introduction

Along with the ribbed vault, the flying buttress is one of the most emblematic Gothic architectural elements. Theoretically, it fulfils three functions (Tarrio 2015; Blas 2018): a) it has an aesthetic purpose and a great visual impact on the outside of the building, b) it drains and channels rainwater from the roof owing to its location and inclination, and, c) it neutralises the horizontal thrusts from the ribbed vaults of the central nave and transmits them to the culées. Despite the above and the many scientific papers and analysis dealing with the functionality of this architectural element (Courtenay 1997, Kimpel and Suckale 1985; Llopis-Pulido, Alonso, Fenollosa, et al., 2016; Roca, Cervera, Pelà, et al., 2013), the fact is that some flying buttresses partially do not fulfil one of the above three functions.

The aesthetic features and the drainage and channelling function can be determined by referring to papers and analysis (Samper, Herrera and Costa-Jover 2022;

Samper, Martín-Sáiz and Herrera 2022) on the shape of these architectural elements, and also by visually examining each element. However, assessing the structural function is not a straightforward task, as it requires a rigorous analysis of the mechanics involved. For this reason, the present paper will attempt to establish an objective method to determine the level of influence of a flying buttress on the overall structural behaviour of the cathedral. In other words, we aim to answer two questions: First, what is the mechanical capacity of a flying buttress?; and second, is this capacity relevant to the overall structural behaviour in the cathedral context? To do so, the present analysis is applied to one of the flying buttresses located at the apse of Girona Cathedral due to its unique features.

The flying buttresses of Girona Cathedral are worthy of study for two reasons. First, these flying buttresses are aesthetically different from any other type of flying buttress, even those located in other cathedrals nearby which historically conditioned the construction process of Girona cathedral. For instance, the strong geographic, historical and constructive influence of Narbonne Cathedral on the architectural design of Girona Cathedral (Freigang 2002; Molina 2007; Cassanelli 1995) fades out when formally comparing both types of flying buttresses. The second reason is that, as shown in Figure 1, the flying buttresses in Girona Cathedral do not fulfil the function of draining rainwater away from the roof. Given the differences in aesthetics, the nonconformity to the usual shape and the absence of a rainwater drainage function, the authors were motivated to evaluate the purpose and structural function of this particular flying buttress.

Figure 1. On the left, a picture showing some flying buttresses of Girona Cathedral. On the right, a picture showing some flying buttresses of Narbonne Cathedral. Despite the geographical, historical and architectural influences, there are significant aesthetic differences. Moreover, the flying buttresses in Narbonne, unlike those in Girona, have the function of draining rainwater. (Pictures by the authors).

In addition to providing an objective method for quantifying the mechanical function of a flying buttress, the aim of this paper is to analyse the specific case of a flying buttress in Girona Cathedral and to check whether its presence contributes to the transmission of thrusts from the vault; in other words, to ascertain whether and to what extent functional aspect c) is fulfilled.

1.1 The flying buttresses of Girona Cathedral as a case study

As described in the previous section, the flying buttresses of Girona Cathedral deserve close consideration due to a) the uniqueness of their aesthetic function and b) the absence of a rainwater drainage function. Moreover, if we compare them with other flying buttresses (Figure 2), we could intuitively suggest, before doing any calculations, that their mechanical function is not particularly important. This intuition is based on

three observations: their angle of inclination is less steep, their resistant section is smaller than is usual for most flying buttresses, and their culées lack a pinnacle (Figures 2 and 3).

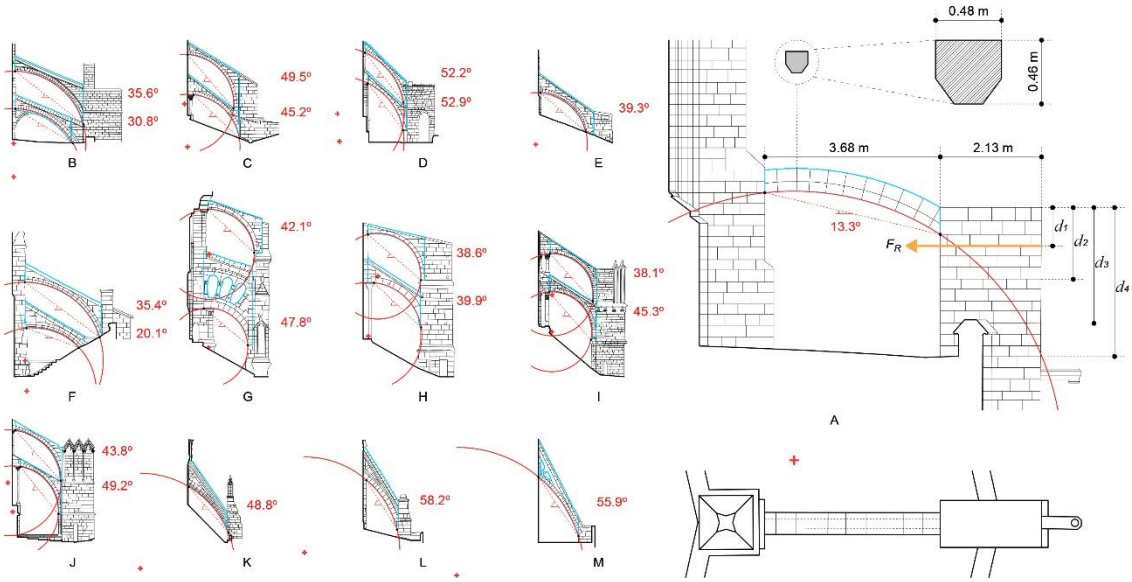

Figure 2. Elevation views of some flying buttresses from 13 cathedrals in different countries, namely 6 Spanish cathedrals (A: Girona Cathedral, B: Mallorca Cathedral, C: Burgos Cathedral, D: León Cathedral, E: Oviedo Cathedral and F: Toledo Cathedral), 4 French cathedrals (G: Chartres Cathedral, H: Saint Pierre church in Chartres, I: Amiens Cathedral and J: Reims Cathedral) and 3 English cathedrals (K: Salisbury cathedral, L: Wells cathedral and M: Bath cathedral). The angle of inclination of each flying buttress is shown in red, and the part of the flying buttress between the cathedral façade and the culée is highlighted in blue. (Pictures by the authors).

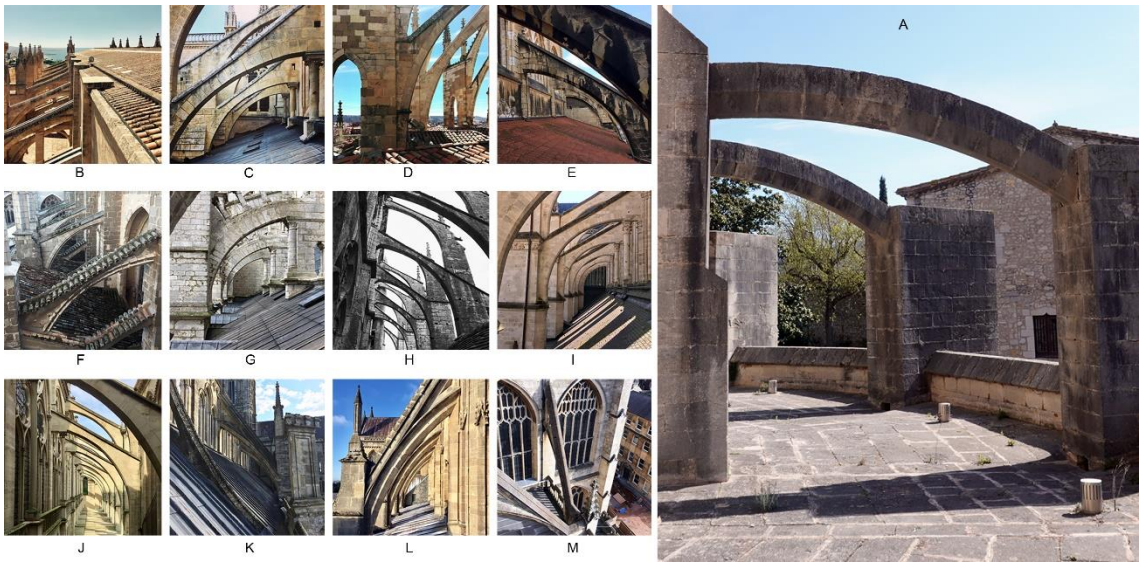

Figure 3. Photographs of some flying buttresses from 13 cathedrals in different countries, all arranged according to the alphabetical order used in Figure 2. (Pictures by the authors).

The ambulatory at the apse of Girona Cathedral is made up of ten flying buttresses. Figure 4 shows the sector which has been isolated to carry out the analysis. According to the reference (Sureda 2005), the analysed flying buttress is located above the chapel that was first built.

Before determining - in the following section - whether or not the mechanical capacity of a particular flying buttress is relevant to the behaviour of the overall structure, graphic statics techniques will be used to calculate a) the maximum mechanical capacity of the flyer arch under consideration as a function of its geometric shape and its construction material; and b) the mechanical capacity of the culée. In order to determine the geometric shape of the flyer arch, a two-dimensional vector drawing of its elevation was made taking into account all its constructive features, i.e. the shape and actual size of the voussoirs forming the arch (Figures 2 and 5). In order to determine the weight of the flyer arch, a value of 26.43 kg/m^3 was used for the density of the stone (nummulitic limestone from Girona). This physical value was taken from the technical

report of a project for damage diagnosis and proposals for intervention on the stone of Girona Cathedral, carried out in 1999 by the Department of Petrology and Geochemistry of the University of Oviedo and commissioned by the Girona Cathedral itself.

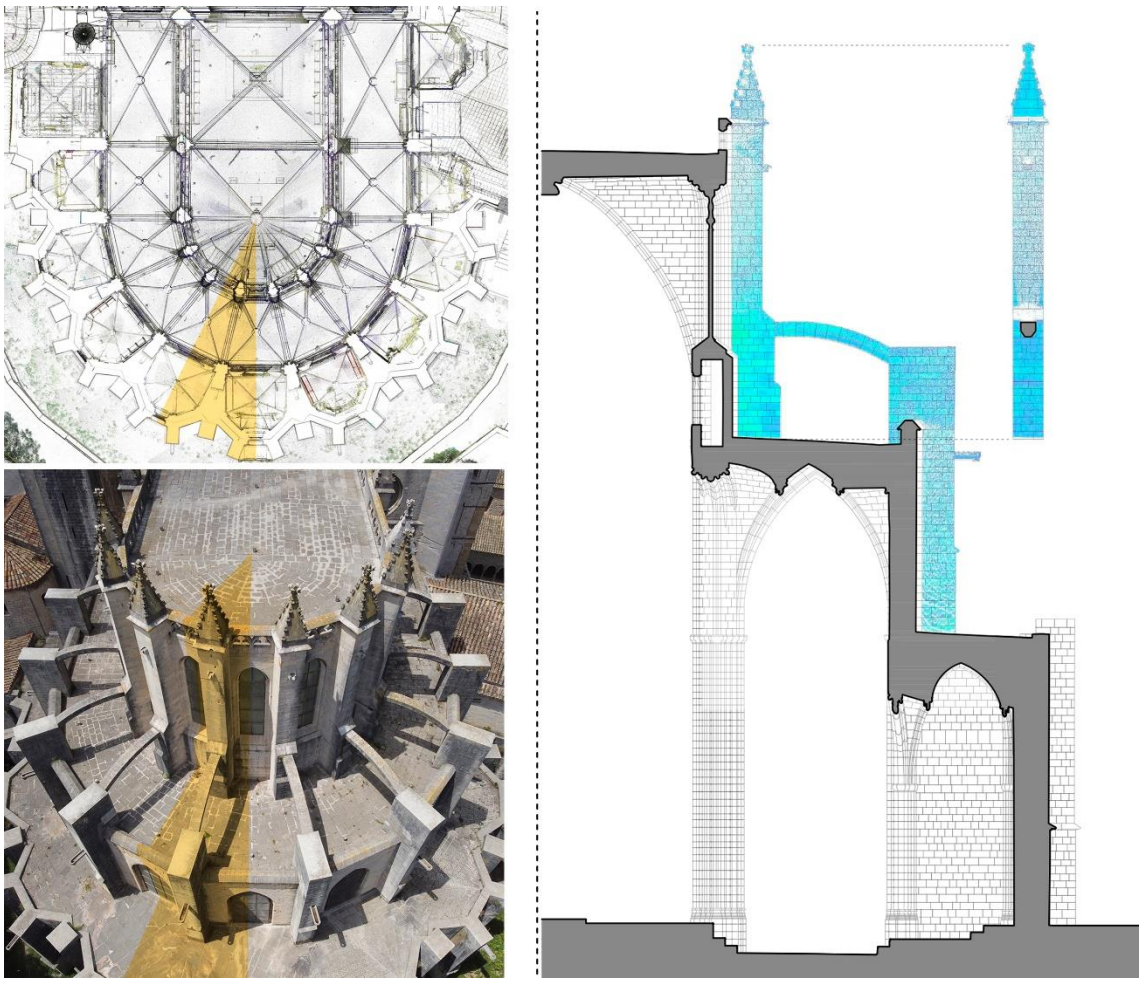

Figure 4. Image of the point cloud generated by using terrestrial laser scanning technology. This figure shows the flying buttresses that make up the ambulatory of Girona Cathedral. The analysed sector is highlighted in orange. (Pictures by the authors).

1.1.1 Analysis of the maximum mechanical capacity of the flying buttress under consideration

Since the geometric shape of this flying buttress of Girona Cathedral is that of a circular semi-arc with the keystone at almost the same height as the top end of the flyer arch, we have assumed that the reaction force at this end is practically horizontal. Thus, four funicular polygons have been inscribed in the plane of the flyer arch: two of them run within the limits of the middle third of the section and generate a maximum and minimum thrust (Figure 5B and Figure 5C, respectively); and the other two run within the physical boundaries of the arch of minimum thickness (Alexakis and Makris 2014; Huerta 2019) and generate a minimum and maximum thrust (Figure 5A and Figure 5D, respectively). In the first two cases, the transmission of forces between the voussoirs always takes place within the limits of the central core, and therefore all fibres are always under compression. In the other two cases, the transmission of forces between the end voussoirs takes place outside the central core, at the physical boundaries of the flyer arch.

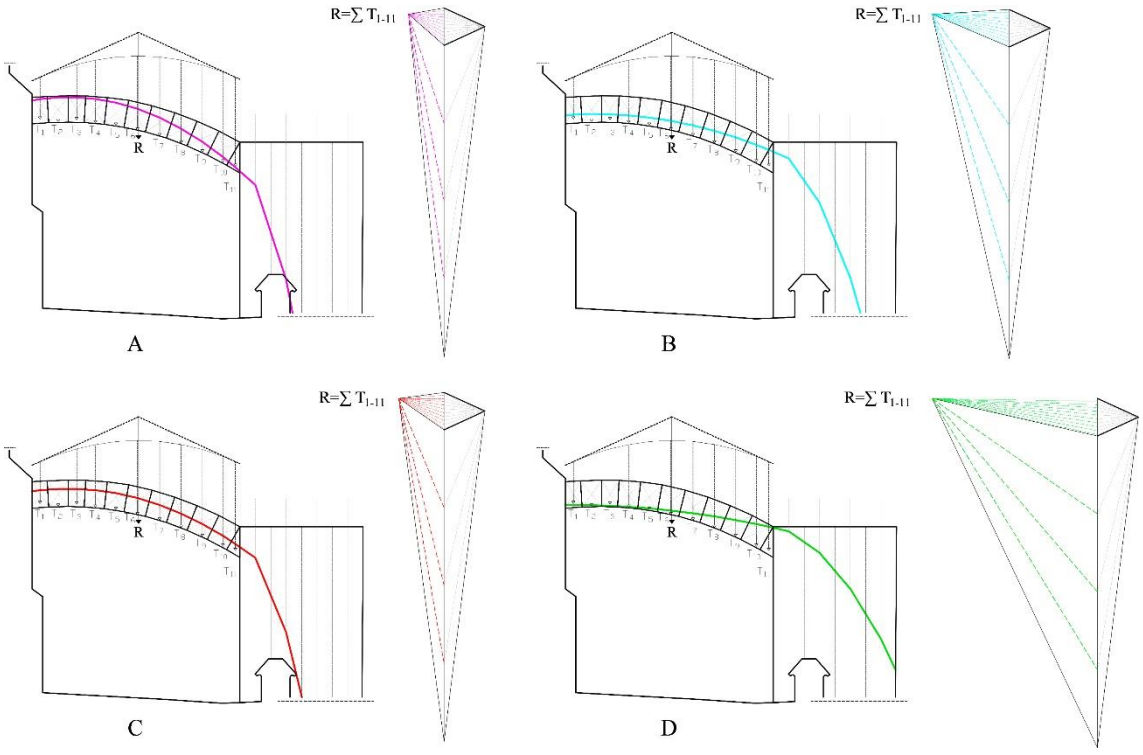

Figure 5. Results of applying the graphic static techniques to the flying buttress from Girona cathedral. Left to right and top to bottom: A) funicular polygon corresponding to the line of minimum thrust within the limits of the minimum thickness arch, B) funicular polygon corresponding to the line of maximum thrust within the limits of the central core, C) funicular polygon corresponding to the line of minimum thrust within the limits of the central core, and D) funicular polygon corresponding to the line of maximum thrust within the limits of the minimum thickness arch.

The graphic static analysis (Figure 5D) shows that the resultant force generated by the maximum thrust goes beyond the limits of the culée. This circumstance is explained in subsection 1.1.2.

In order to calculate the value of the thrust forces R_H corresponding to each funicular polygon and the vertical reaction at the lower end R_V, the area in elevation of each voussoir is multiplied by the average thickness of the flyer arch and by the density of the stone (Table 1).

Acronym	**Funicular polygon shape**	**R_H (KN)**	**R_V (KN)**	**Figure**
(MaxT-MTA)	Maximum thrust Minimum thickness arch	90.52		5D
(MaxT-CC)	Maximum thrust Central core	42.23	23.30	5B
(MinT-CC)	Minimum thrust Central core	24.82		5C
(MinT-MTA)	Minimum thrust Minimum thickness arch	19.52		5A

Table 1. Horizontal and vertical reaction forces at the ends of the flyer arch according to the four funicular polygons described above.

It follows from all of the foregoing that the horizontal reaction forces due to the self weight of the flyer arch can vary between 19.52 and 90.52 KN.

1.1.2 Analysis of the maximum mechanical capacity of the culée under consideration

Continuing with the calculation of the mechanical capacity of the culée, we find that the capacity to absorb the horizontal reaction force is limited by the frictional force F_R that could be generated at the horizontal joint between the stone courses of the culée which are located just below the lower end of the flyer arch (Figure 2). This frictional force F_R is directly proportional to the friction coefficient μ and to the vertical force F_V at the joint. Because the flyer arch starts at the top of the culée and there is no pinnacle, the vertical force F_V on this joint, and therefore the frictional force, is very limited. This frictional force has been calculated considering the weight of three stone courses of the culée (Figure 2 and Figure 5), in addition to the vertical reaction force of the flyer arch, and also considering different friction coefficients for stone masonry walls (Rankine 1858; Vasconcelos and Lourenço 2009; Milosevic, Sousa Gago, Lopes, et al., 2013). In order to calculate the weight of the last three stone courses of the culée, we have taken into account their dimensions (3 x 0.26 x 2.10 x 0.98 m) and the density of the Girona limestone (26.43 KN/m3), although it is true that the weight could be slightly lower depending on the heterogeneity in the composition of the materials.

F_V (KN)	μ	F_R (KN)	Acronym
23.30 (flyer arch) + 42.43 (culée)	0.60	39.43	(LFLC)
	0.70	46.01	
	0.74	48.63	
	0.78	51.26	(HFLC)

Table 2. Frictional forces F_R in the horizontal plane of the culée joint, directly under the springing of the flyer arch, considering four different friction coefficients μ.

It follows from all of the foregoing that the frictional force that could be generated between the stone courses of the culée, directly under the springing of the

flyer arch, is between 39.43 KN (LFLC, lowest friction limit of the culée) and 51.26 KN (HFLC, highest friction limit of the culée). This means that a horizontal reaction force of the flyer arch in excess of these values would cause a displacement of the courses and a collapse of the flyer.

Of the four thrust forces which have been calculated using graphic static techniques, only two are lower than the maximum friction forces that could occur at the culée; specifically, they correspond to the line of minimum thrust within the limits of the minimum thickness arch and the line of minimum thrust within the limits of the central core (Figure 5A and Figure 5C, respectively).

The horizontal force itself generates an overturning moment on the culée which is directly proportional to the vertical distance *d* considered. This moment is counteracted by a balancing moment M_e which is also directly proportional to the weight of the flying buttress $R_{V,f}$ and the weight of the culée $R_{V,b}$ according to the same distance *d* considered. From these values, it is possible to infer the maximum horizontal force $F_{H,max}$ that would cause the buttress to overturn considering different vertical distances (Table 3). This force varies from 119.84 kN (at the level directly below the springing of the flyer arch) to 72.80 kN (MOFC, maximum overturning thrust) approximately 3 m beneath that (Figure 2). In any case, these forces are not limiting, as they are greater than the forces which would be the cause of the displacement imbalance calculated above.

***d* (m)**	**$R_{V,f}$ (KN)**	**$R_{V,b}$ (KN)**	**M_e (KNm)**	**$F_{H,max}$ (KN)**	**Acronym**
d_1 = 0.78	23.30	42.43	93.48	119.84	
d_2 = 1.56		84.85	138.03	88.48	
d_3 = 2.34		127.28	182.57	78.02	
d_4 = 3.12		169.71	227.12	72.80	(MOFC)

Table 3. Maximum horizontal forces $F_{H,max}$ that would cause overturning with different vertical distances *d* measured from the top of the culée (Figure 2).

In summary, the flying buttress-culée unit is capable of absorbing horizontal thrusts within a minimum range from 19.52 KN (MinT-MTA) to 39.43 KN (LFLC) and a maximum range from 19.52 KN (MinT-MTA) to 51.26 KN (HFLC). Specifically, the first value of each interval corresponds to the minimum thrust produced by the flyer arch considering the limits of the minimum thickness arch (Figure 5A and Table 1) and the second value corresponds to the minimum and maximum frictional resistance that would be present at the culée stone course located directly below the springing of the flyer arch (Table 2).

2. Analysis of the mechanical capacity of a flying buttress and its structural relevance

Once the mechanical limits of the flying buttress and its culée have been calculated, the following section describes a method for determining the mechanical capacity of the flying buttress taking into account its architectural context. For this reason, this section is divided into two subsections: the first subsection presents the steps to follow in order to three-dimensionally model the architectural context of the flying buttress under consideration; the second subsection presents the steps to follow in order to assess the mechanical capacity of the culée by means of a simulation. As already stated, the following procedures are applied to a specific flying buttress located in Girona Cathedral.

2.1 Obtaining a geometrical model of the study object

First of all, a three-dimensional digital model of the study object was created. For this purpose, the terrestrial laser scanner Leica RTC360 was used, with an accuracy of less than 2 millimetres. The three-dimensional numerical data were processed using the Cyclon Register 360 software and the Cyclone software. This modelling process is non-invasive to the architectural heritage and is often used for graphic representations

due to its high operating speed and simplicity (Grussenmeyer, Landes, Voegtle et al., 2008).

This method of representation has made it possible to determine with millimetre precision the current state of the entire apse of the Cathedral and in particular the sector under consideration, which is shown in Figure 6.

In order to proceed with the following steps in this subsection, the point cloud corresponding to the sector under consideration was transformed into a three-dimensional mesh. Specifically, from a cloud of 397,356,684 points, a second model emerged, made up of 5,099,321 polygonal shapes. In order to reduce the file size of the second model to a minimum, without altering its geometry, a third model was created using the Autocad software. Figure 6 shows these geometric transformations.

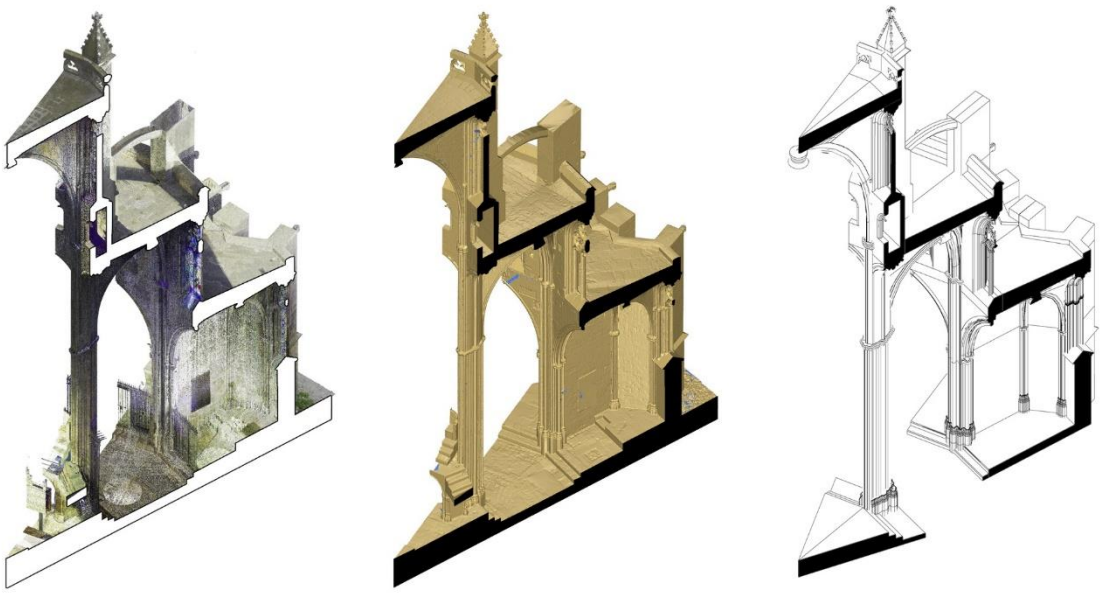

Figure 6. On the left, a part of the point cloud obtained with the laser scanner and registered with the Cyclone software. In the centre, the three-dimensional mesh for this sector, which was created with the Cyclone 3DR software. On the right, the third model generated with AutoCad software.

2.2 Assessment of the structural relevance of the flying buttress

In this subsection, we quantify the magnitude of the stress to which the flying buttress is subjected, taking into account all the stiffness values of the architectural elements in the analysed sector. This calculation is applied to an analysis model (model A). Once this magnitude is known, and in order to assess the mechanical contribution of the flying buttress to the structure as a whole, the calculations are applied to an alternative analysis model (model B) where the flying buttress is not present.

2.2.1 Rendering of the simulation model

The *Autodesk Robot Structural Analysis* software and the third geometric model mentioned in subsection 2.1 are used to continue with the structural analysis using the finite element method (FEM). To do this, it was necessary to create a new simplified geometric model, made up of planes and lines (Figure 7), on which we will carry out the calculations to define the mechanical differences between the analysis models A and B. This simplification process was carried out on the following basis:

- The median planes of the walls and the axes of the ribs were considered.
- The curvature of the ribs was modelled using polygonal lines.
- The geometry of the pilasters and columns was simplified to an equivalent rectangular cross-section. (Figura 7A).
- In order to define possible horizontal fracture planes, a horizontal joint was considered for each three stone courses. (Figure 7B)
- Vertical joints were not considered in general, but only in those areas where this has been necessary to obtain a mechanical behaviour which is comparable to a real compression-only behaviour by introducing disconnections between elements.

- In order to simulate the interaction with the adjacent sectors, supports were introduced with limited displacement in the horizontal plane and free displacement in the vertical direction.
- In addition, at the ends of the bars and panels that are in touch with these supports, spin releases and transverse displacement releases were introduced, so that the reactions on these supports are only compressive forces in the horizontal plane (Figure 7C).
- The modulus of elasticity *E* of stone masonry can vary between $1.7x10^{-3}$ and $6.85x10^{-3}$ N/mm^2 (Magenes, Penna, Galasco, et al., 2010; Gonen and Soyoz 2021). This variability is not only due to the constructive heterogenity, but also to the diversity of the methods used to characterise the modulus of elasticity. This disparity in values implies uncertainty in the analysis model and its results, in particular the resulting values of displacements and deformations. For this reason, these results should not be interpreted as absolute and precise. They only provide an order of magnitude. For all the above reasons, and because the constructive heterogeneity of the walls is greater than that of the ribs, different moduli of elasticity were applied to these two elements; specifically, 2x10-3 and 4x10-3 KN/mm2, respectively.
- The wall panels were discretised into a mesh of three- and four-node elements no larger than 30 centimetres in size, and a denser mesh with 10-centimetre elements was used in areas where there is greater unevenness or higher stress concentrations.

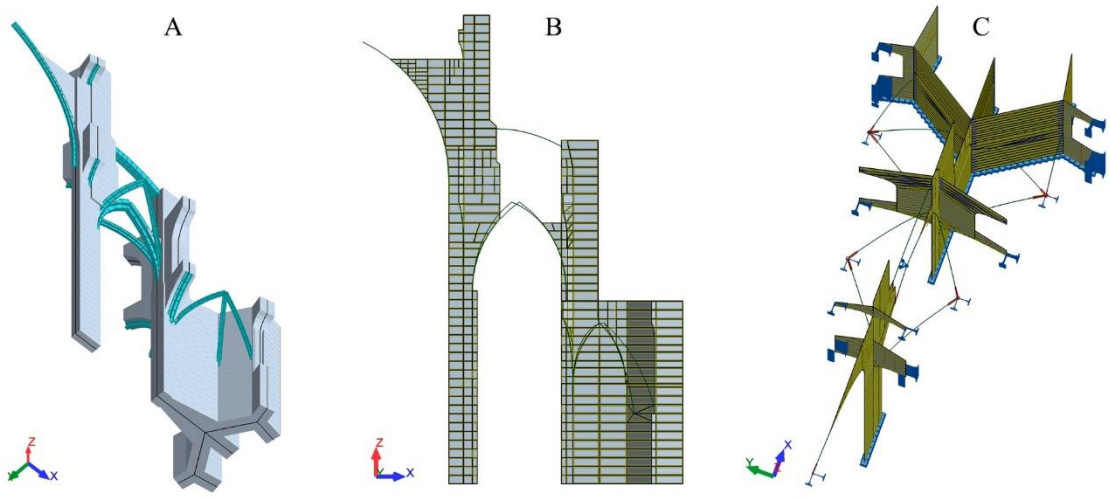

Figure 7. Three graphical representations of the FEM model. Left to right: A) Axonometric view showing wall and rib thicknesses; B) Cross-section of the model showing the wall panels and the horizontal joints; C) Axonometric view showing supports and releases at the ends and edges of elements which are in contact with adjacent sectors.

In general in FEA, materials characterisation is a greater source of uncertainty than geometric characterisation. If materials characterisation has been carried out by means of tests, it will be possible to obtain values closer to reality. Otherwise it will always be necessary to resort to bibliographic values (Magenes, Penna, Galasco, et al., 2010; Gonen and Soyoz 2021).

2.2.2 Determination of loads on vaults

The following is a description of all the considerations that the authors made in order to optimally determine the loads on the vaults:

- The loads due to the self-weight of walls, pilasters, columns, arch ribs, vaults and earthenware infill were taken into account. A density of 26.43 Kg/m^3 was considered for all stone elements and a density of 18.00 Kg/m^3 was considered for the vault's earthenware infill.

- To estimate the weight of the vaults themselves, a constant thickness of 30 centimetres was assumed; also, to estimate the volume of the earthenware infill, the tributary area in plan was multiplied by the vertical distance from each rib point to the top horizontal plane of each vault (Figure 8).

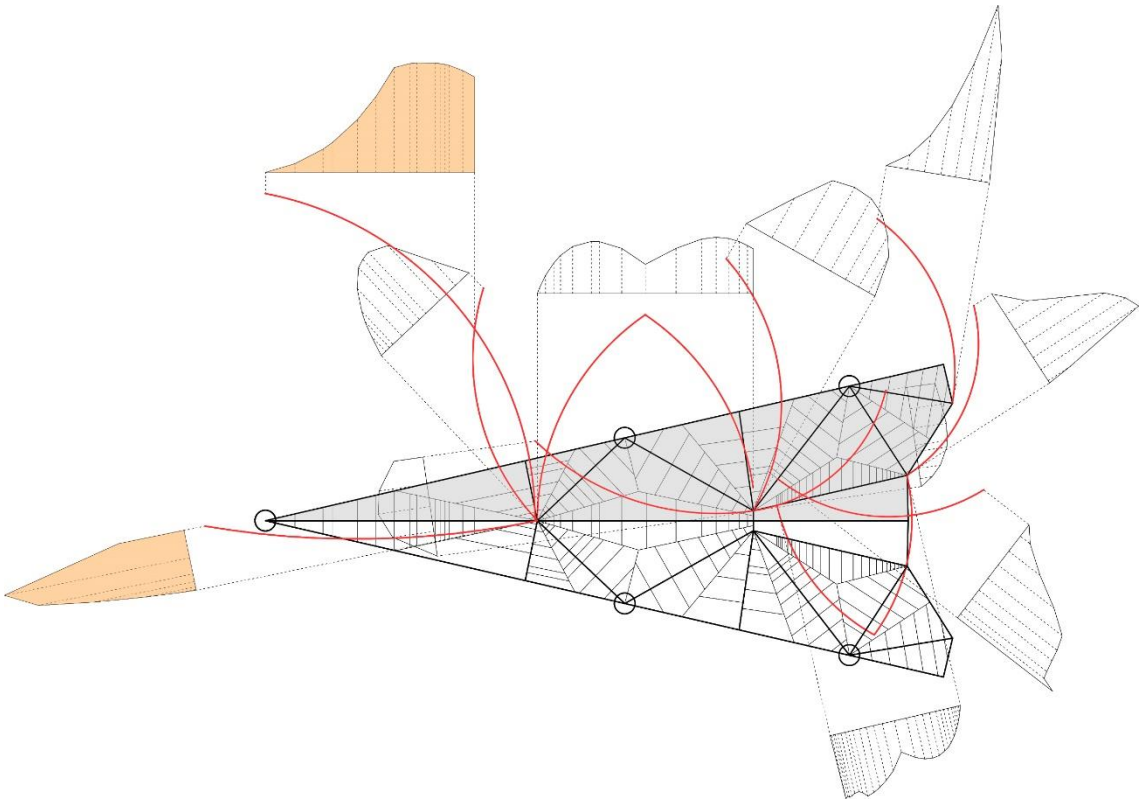

Figure 8. Diagram showing the tributary areas in plan and cross-section which were used to estimate the loads on the vault ribs. The loads on the vaults of the central nave are highlighted in orange.

2.2.3 Considerations on the building stages and loading of the flying buttress

No construction element can be affected by loads that started to act before that element was built. According to this premise, the elements of the cathedral were built and loaded following an ascending order. Thus, the elements at a lower level are affected by all the loads resulting from the weight of the elements above them. Similarly, the elements at the top of the cathedral are only affected by their self-weight and the weight of the materials resting on them. In any case, the stiffness of the overall

structure is important at all building stages. In other words, the behaviour of the elements built in a given stage is not influenced by the loads which were present at a previous stage, but is influenced by the stiffness of the elements which have already been built.

We do not know in detail the building and loading chronology of the elements which are present in this sector of the apse, but we can hypothesise that the logical order was as follows: the side chapels were built first, then the ambulatory nave and finally the central nave with the culée and the flying buttress (Fig. 9). For the purposes of this analysis, it is assumed that the vaults were filled in at the same time as, or immediately after, the vaults themselves were built. According to this hypothesis, the behaviour of the flying buttress and the upper part of the culée were influenced by the weight of the elements which were built in the third stage and by the stiffness of all the elements built during the three stages.

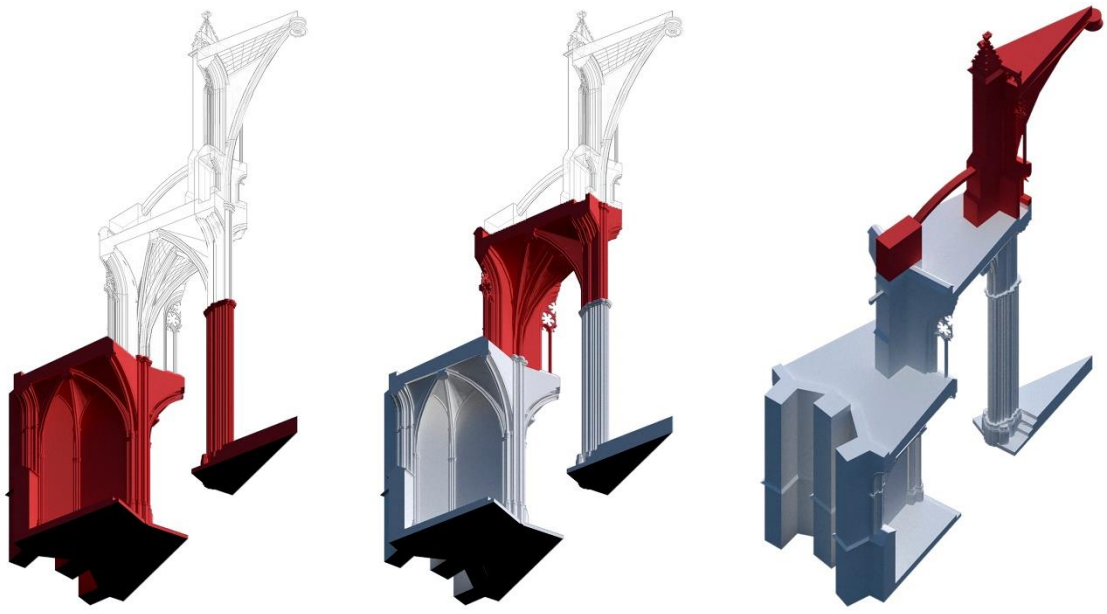

Figure 9. Hypothesis on the building stages and loading of architectural elements. On the left, first building stage; in the centre, second building stage; and on the right, third building stage.

2.2.4 Obtaining a compression-only structural behaviour

A Finite Element Method (FEM) simulation has a mechanical behaviour which is equivalent to that of the real structure when the dominant force is a compression force, with residual tension forces and bending moments. This behaviour is achieved by the systematic introduction of discontinuities between elements in areas where tension forces are present in the initial calculation. This process of introducing discontinuities was repeated until a behaviour without relevant tension forces was obtained. (Figure 10). In other words, the stone masonry of the walls was considered to be a set of elastic elements which are separated by potential fracture lines (López, Oller and Oñate 1998).

3. Results

The FEM analysis of Model A has made it possible to evaluate the magnitude order of the forces and displacements of the flyer arch and the adjacent walls which are subjected to the self-weight of the elements built in the third building stage (Figure 9). With model A, the compression force at the lower end of the flyer arch is 29.35 KN, which translates into a horizontal thrust of 28.83 KN (Figure 10). This value is slightly higher than the minimum thrust obtained by graphic statics and presented in subsection 1.1.1.

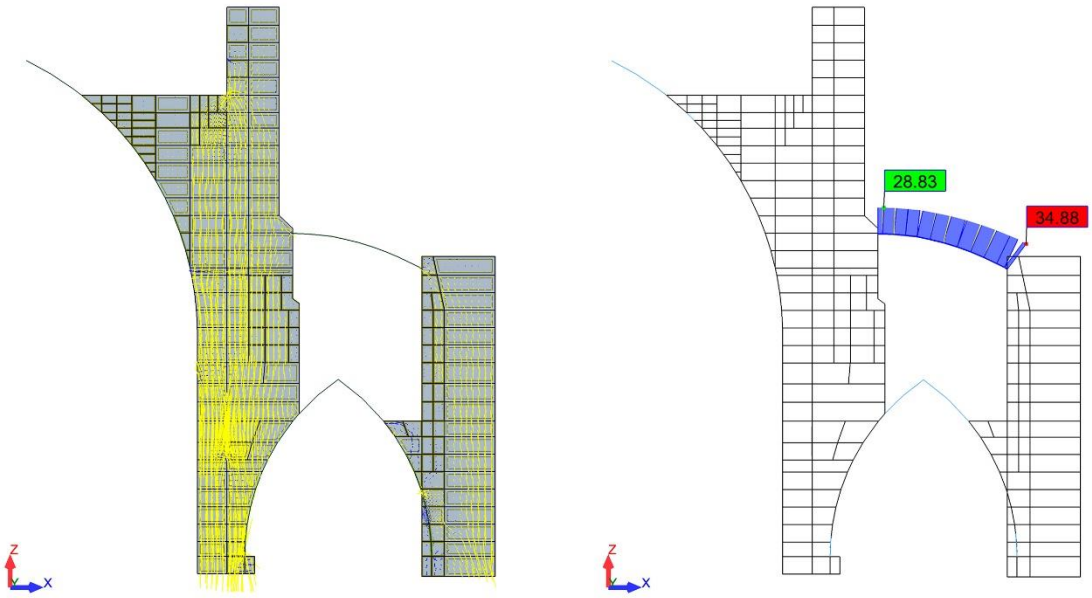

Figure 10. Images of the FEM analysis model A: on the left, the compression force vectors of the thrust lines on the walls of the upper part of the analysed sector; on the right, the axial compression force on the flying buttress due to the self-weight of the elements built in the third stage.

In order to evaluate the impact of the flying buttress on the mechanical behaviour of the structure as a whole, the horizontal displacements obtained in model A were compared with the displacements that would be obtained in an identical model B lacking the flying buttress.

In model A (Figure 11) it can be seen that the horizontal displacement at the lower end of the flyer arch, next to the culée, is greater than the horizontal displacement at the upper end. The difference of almost 2 millimetres between the two ends results in a slight increase in the length of the flying buttress. In other words, due to the limited stiffness of the culée, there is a difference in displacement of approximately 2 mm. This difference in displacement is probably one of the reasons why the horizontal thrust of the flying buttress is close to the minimum required for stability. Greater stiffness of the culée, based on the application of a higher modulus of elasticity than that considered in

this model, would reduce this differential displacement and increase the horizontal force transmitted by the culée. Even if a higher modulus of elasticity is considered, the horizontal thrust should never reach the limit of 51.26 KN, as this value is the limit of the sliding resistance of the stone courses at the top of the culée.

In model B (Figure 11), it can be seen that the horizontal displacements of the central nave wall at the level of the flying buttress are slightly higher (between 20 and 25% approximately) than in model A. This difference indicates a certain efficiency in the structural function of the flying buttress to avoid horizontal deformations due to the thrust of the central nave.

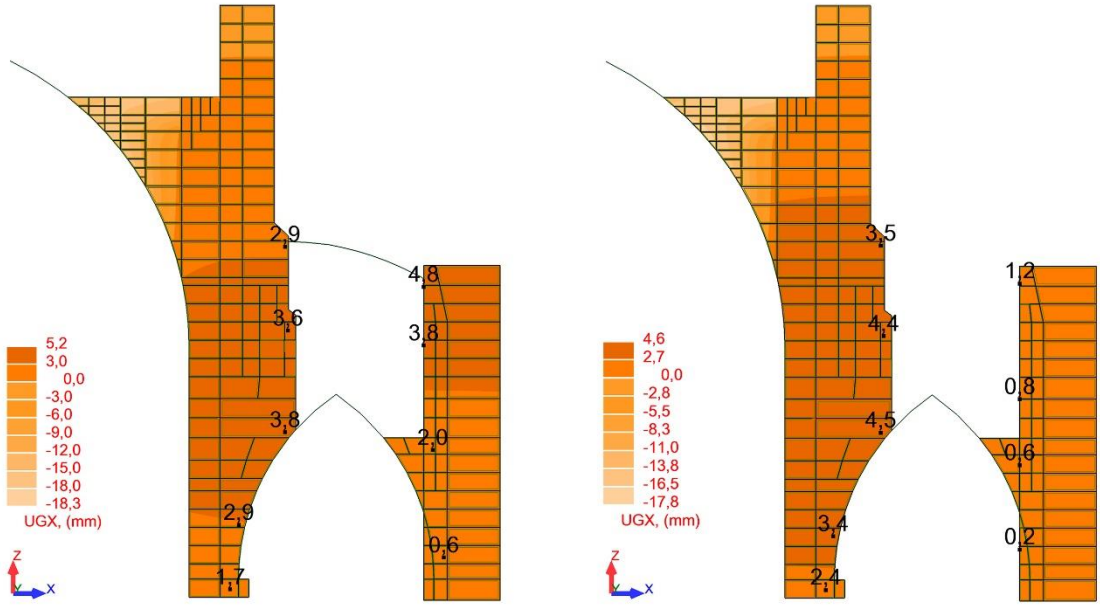

Figure 11. Horizontal displacements of FEM analysis models A and B: on the left, the effect of the flying buttress is taken into account; on the right, the effect of the flying buttress is not taken into account.

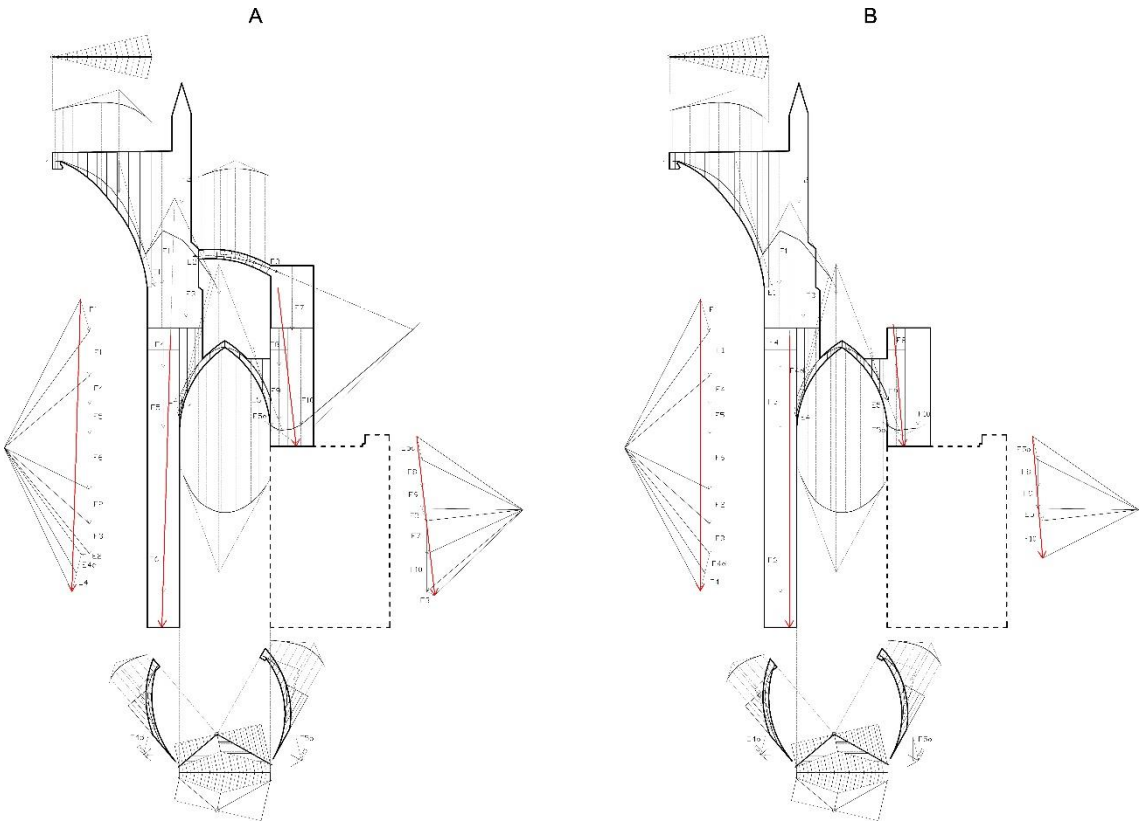

Figure 12. Graphic statics analysis of the sector under consideration for models A and B.

To corroborate the above results, a graphic statics analysis of the sector under consideration is shown for models A and B (Figure 12). This analysis shows how the position and inclination of the resultant force changes depending on the presence or absence of the culée and the flying buttress.

4. Conclusions

This paper establishes an objective method to determine the mechanical capacity of a flying buttress and to assess its structural relevance in the cathedral context.

By applying this method of structural analysis to one of the flying buttresses of Girona Cathedral, its mechanical capacity was determined, considering the minimum and maximum thrusts that can be assumed by the flyer arch itself and the culée. From this mechanical capacity, using the method presented in Section 2 and taking into

account the loading order of the elements according to their building stages, new stress values were obtained that can be compared with the range of maximum and minimum thrusts which are inherent to the mechanical capacity of the flying buttress and its culée, as shown in Figure 13.

Thus, on the basis of the horizontal displacements obtained in models A and B, it can be seen that the flying buttress and its culée have little structural relevance. Furthermore, the graphic statics analysis presented in Figure 12 shows that the position of the resultant force at the base of the column varies with the presence or absence of the culée, but does not affect the stability of the ensemble. This method shows that function c) of the analysed flying buttress (neutralising and transmitting horizontal thrusts to the culée) is of little relevance in this particular case.

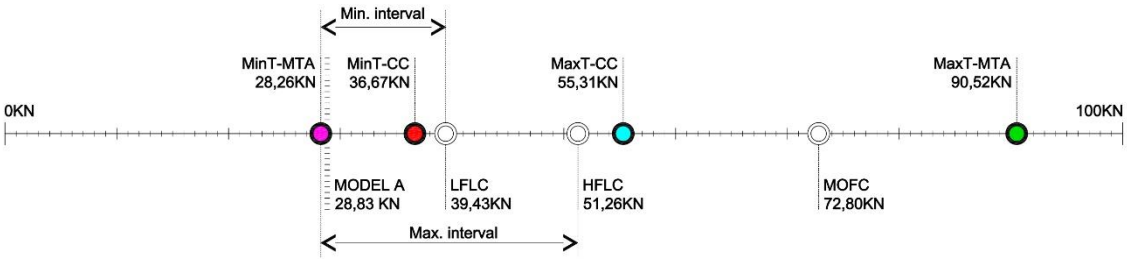

Figure 13. Graphic representation of the thrust values resulting from the analysis of the flying buttress of Girona Cathedral. This figure summarises the most representative values of the tests carried out and indicates the minimum and maximum intervals at which the buttress and culée unit would be stable. Pink color refers to Minimum thrust Minimum thickness arch (MinT-MTA), red colour refers to Minimum thrust Central core (MinT-CC), blue colour refers to Maximum thrust Central core (MaxT-CC) and green colour refers to Maximum thrust Minimum thickness arch (MaxT-MTA).

5. References

Alexakis, H., N. Makris. 2014. Limit equilibrium analysis of masonry arches. Archive of Applied Mechanics. 85(9): 1363-1381.doi: 10.1007/s00419-014-0963-6.

Blas, A. 2019. El puntal de piedra, estática y estética del arbotante gótico. Madrid: Universidad Politécnica de Madrid.

Cassanelli, R. 1995. Talleres de arquitectura en la edad media. Barcelona: Moleiro.

Courtenay, L. 1997. The engineering of medieval cathedrals. 1st ed. London: Routledge.

Freigang, C. 2002. La catedral de Narbona com a referent directe de les Barcelona i Girona, L'art gòtic a Catalunya. Arquitectura I: catedrals, monestirs i altres edificis religiosos. 1st ed. Barcelona: Enciclopèdia Catalana.

Huerta, S. 2019. El arco límite: breve historia de un problema estructural. Paper presented at XXI Congreso Nacional de Historia de la Construcción. Soria, Spain. October 9-12.

Gonen, S., S. Soyoz. 2021. Investigation on the elasticity modulus of stone masonry. Structures. 30: 378-389. doi: 10.1016/j.istruc.2021.01.035.

Grussenmeyer, P., Landes, T., Voegtle, T., and Ringle, K. 2008. Comparison methods of terrestrial laser scanning, photogrammetry and tacheometry data for recording of cultural heritage buildings. The International Archives of the Photogrammetry, Remote Sensing and Spatial Information Science 37:213-18.

Kimpel, D., and R. Suckale. 1985. Die gotische Architektur in Frankreich: 1130-1270. München: Hirmer Verlag.

Llopis-Pulido, V., A. Alonso, E. Fenollosa, and A. Martínez. 2016. Análisis constructivo y estructural de la catedral de Valencia. Informes de la Construcción 68 (543):1-10. doi: http://dx.doi.org/10.3989/ic.15.102.

López, J., S. Oller, and E. Oñate. 1998. Cálculo del comportamiento de la mampostería mediante elementos finitos. Barcelona: CIMNE.

Magenes, G., A. Penna, A. Galasco and M. Rota. 2010. Experimental characterization of Stone masonry mechanical properties. Paper presented at the 8th International Masonry Conference. Dresden, Germany. July 4-8.

Milosevic, J., A. Sousa Gago, M. Lopes and R. Bento. 2013. Experimental assessment of shear strength parameters on rubble masonry specimens. Construction and Building Materials. 47: 1372-1380. doi: 10.1016/j.conbuildmat.2013.06.036.

Molina, F. 2007. De genere militari ex utroque parente. La nobleza eclesiástica y los inicios de la Catedral Gótica de Gerona. Anuario de estudios medievales 37 (1):741-780. doi: https://doi.org/10.3989/aem.2007.v37.i2.52.

Rankine, W. J. M. 1858. Manual of applied mechanics. London: C. Griffin and Co.

Roca, P., M. Cervera, L. Pelà, R. Clemente, and M. Chiumenti, 2013. Continuum FE Models for the Analysis of Mallorca Cathedral. Engineering Structures 46: 653-670. doi: http://dx.doi.org/10.1016/j.engstruct.2012.08.005.

Samper, A., B. Herrera and A. Costa-Jover. 2022. Systematic calculation of flying buttress parameters by means of geometric regression. Journal of Cultural Heritage 54: 21-30. doi: https://doi.org/10.1016/j.culher.2022.01.005.

Samper, A., R. Martín-Sáiz and B. Herrera. 2022. On the inclination of a flying buttress arch. Nexus Network Journal 24: 897-911. doi: https://doi.org/10.1007/s00004-022-00619-7.

Sureda, M. 2005. Catedral de Girona. Barcelona: Ediciones Aldeasa.

Tarrío, I. 2015. Los arbotantes en el sistema de contrarresto de construcciones medievales: teorías sobre su comportamiento estructural. In Actas del Noveno Congreso Nacional y Primer Congreso Internacional Hispanoamericano de Historia de la Construcción, 1675-85. Segovia: Instituto Juan de Herrera.

Vasconcelos, G. and P. B. Lourenço. 2009. Experimental characterization of stone masonry in shear and compression. Construction and Building Materials. 23(11): 3337-3345. doi: 10.1016/j.conbuildmat.2009.06.045.

6. Acknowledgment

The survey of the Cathedral of Girona was financed by the Capítol Catedral de Girona through the project T19243S - Aixecament topogràfic de la Catedral de Santa Maria de Girona.

7. Funding

This work is part of the research project “Smart Built Heritage. Del registro a la simulación digital para inmuebles medievales y modernos” with reference TED2021-129148B.